Tight-binding polarons. II. The interstitial-polaron model

1989 J. Phys.: Condens. Matter 1 3897

(http://iopscience.iop.org/0953-8984/1/25/002)

J. Phys.: Condens. Matter 1 (1989) 3897–3910. Printed in the UK

Tight-binding polarons: II. The interstitial-polaron model

A Klamt†
Max-Planck-Institut für Metallforschung, Institut für Physik, Heisenbergstrasse 1, D-7000 Stuttgart-80, Federal Republic of Germany

Received 20 September 1988, in final form 17 November 1988

Abstract. The present paper is concerned with the problem of the polaronic states of positively charged particles in crystals. In contrast to the commonly considered case of electronic polarons such particles tend to reside on the interstitial sites of the crystal. To work out the consequences of this fact the interstitial-polaron model is investigated. This model is a slight modification of Holstein's molecular-crystal model treated in part I of this series. Using the variational approach introduced in part I a new class of polaronic states appears to become stable in some parameter region in addition to the various types of states existing for the molecular-crystal model. These states will be called two-site states since they describe a particle effectively tunnelling between two neighbouring sites. They are shown to be increasingly important if a configuration dependence of the transfer integral is taken into account. The two-site states may be considered as a one-dimensional analogue of the 4T states which have been proposed for hydrogen and its isotopes in BCC metals.

1. Introduction

The behaviour of light positively charged particles like hydrogen nuclei, positive muons and pions, and positrons in metals and semiconductors has been investigated for about two decades (for a review see Alefeld and Voelkl (1978)). During the last few years the question of a crossover from coherent motion at low temperatures to incoherent hopping at higher temperatures has attracted great experimental and theoretical interest (for a review see Richter (1986)). Up to now the coherent states of these particles have been described using the theoretical concepts developed for electronic polarons. Differences which might arise from the fact that positively charged particles in contrast to electrons prefer to reside on the interstitial sites of a crystal can therefore not be noticed. Numerical calculation on hydrogen isotopes in BCC metals (Sugimoto and Fukai 1981, Klamt and Teichler 1986) strongly suggest that in these systems, especially for very light particles, states delocalised over four tetrahedral sites (4T states) become stable with respect to states localised at a single tetrahedral site (1T states). Owing to lack of translational invariance neither the 1T states nor the 4T states are exact coherent eigenstates of the system. It is straightforward to overcome this lack by construction of coherent polaron solutions starting from localised 1T states using conventional polaron theories. However it is by far uncertain how to construct polaronic 4T states, although these may be the ground states of light positively charged particles in BCC metals.

† Present address: Bayer AG, AV-IM-AM, D-5090 Leverkusen, Federal Republic of Germany.

0953-8984/89/253897 + 14 $02.50

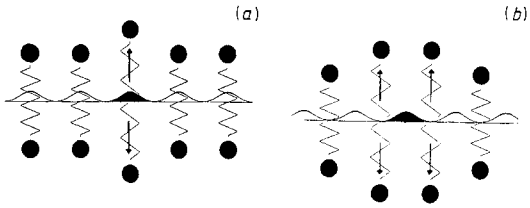

Figure 1. Schematic representation of the polaron models: (*a*) the molecular-crystal model; (*b*) the interstitial-polaron model. The oscillators may be thought of as diatomic molecules. The arrows denote the forces exerted by a particle in the occupied (filled) particle state.

In this paper for the first time an interstitial-polaron model (IPM) will be investigated. The IPM is a slight modification of the molecular-crystal model (MCM) which has been introduced by Holstein (1959a, b) and has been reconsidered by the author in part I of this series concerning tight-binding polarons (Klamt 1988). It will be shown that two-site states (2S states) analogous to the previously mentioned 4T states do in fact appear as stable polaronic solutions despite the simplicity and one-dimensionality of the model.

The paper is organised as follows. First a short description of the IPM will be given. Then the polaronic solutions will be investigated using the powerful variational approach introduced in part I. Thereafter the IPM will be expanded beyond the Condon approximation (CA) by inclusion of a configuration dependence of the transfer integral. Finally the results will be summarised and discussed.

2. The interstitial-polaron model

In his MCM Holstein considered a light particle moving through a linear chain of non-interacting oscillators. The particle states are assumed to be tightly bound to the oscillators. When a particle is occupying such a state it is interacting linearly with the entire oscillator. The MCM is shown schematically in figure 1(*a*). Denoting the reduced mass of one oscillator by M and the oscillator frequency by ω and introducing the oscillator units ω^{-1}, $(\hbar/M\omega)^{1/2}$ and $\hbar\omega$ for time, length and energy, respectively, the Hamiltonian of the MCM has been shown to be

$$H = H_{\mathrm{L}} + H_{\mathrm{P}} + H_{\mathrm{I}}. \tag{1}$$

Here

$$H_{\mathrm{L}} = \tfrac{1}{2}\sum_{\alpha}(-\partial^2/\partial Q_\alpha^2 + Q_\alpha^2 - 1) \tag{2}$$

is the lattice Hamiltonian with Q_α being the degree of freedom of the oscillator α. Denoting the transfer integral by J and using the annihilation and creation operators a_α and a_α^+ for a particle in the localised state φ_α the particle Hamiltonian takes the form

$$H_{\mathrm{P}} = -J\sum_{\alpha}(a_\alpha^+ a_{\alpha+1} + a_{\alpha+1}^+ a_\alpha). \tag{3}$$

Finally in the MCM the linear interaction is described by

$$H_{\mathrm{I}} = -A\sum_{\alpha} Q_\alpha a_\alpha^+ a_\alpha \tag{4}$$

where A is the force acting on the oscillator.

Let us now consider the slightly modified model shown in figure 1(*b*). In this model each particle state φ_α is no longer centred at oscillator α but between the oscillators α

and $\alpha + 1$, i.e. at an interstitial site. We shall call this model the interstitial-polaron model (IPM). While the lattice Hamiltonian as well as the particle Hamiltonian remain the same as in the MCM, the interaction Hamiltonian now takes the form

$$H_I = \sum_\alpha -A(Q_\alpha + Q_{\alpha+1})a_\alpha^+ a_\alpha \tag{5}$$

since a particle in state φ_α now interacts with both its neighbouring oscillators.

Before turning to the variational calculations the two obvious limiting cases will be considered. For vanishing interaction ($A \to 0$) the particle ground state is a simple band state with wavevector k equal 0 and energy $-2J$ as it is in the MCM. On the other hand for vanishing transfer integral J the particle is localised at a single interstitial site and the neighbouring oscillators are displaced by A. The total energy of this state is $-A^2$ compared with $-\frac{1}{2}A^2$ in the MCM.

3. Variational calculations

In this section we look for the ground state of the system using the variational approach introduced in part I. The concepts of this approach will not be discussed here again. The reader therefore should recap on the corresponding chapter in part I. Let us start with the wavefunction

$$\Psi = N^{-1/2} \sum_\alpha e^{ik\alpha} \Psi_\alpha = N^{-1/2} \sum_\alpha e^{ik\alpha} (c\Psi_\alpha^{1S} + s e^{ik/2} \Psi_\alpha^{2S}) \tag{6}$$

where

$$\Psi_\alpha^x = \left(\sum_\beta c_\beta^x a_{\alpha+\beta}^+ \right) |0\rangle \prod_\gamma \{\pi^{-1/4} \exp[-\tfrac{1}{2}(Q_{\alpha+\gamma} - q_\gamma^x)^2]\} \tag{7}$$

for $x = 1S$ and $2S$. Here c and s are the weights of the one-site (1S) and two-site (2S) wavefunctions and

$$c_\beta^{1S} = [(1 - \lambda^2)/(1 + \lambda^2)]^{1/2} \lambda^{|\beta|} \tag{8a}$$

$$q_\beta^{1S} = q \begin{cases} \kappa^{\beta+1} & \text{if } \beta > 0 \\ \kappa^{-\beta} & \text{if } \beta \leqslant 0 \end{cases} \tag{8b}$$

$$c_\beta^{2S} = [(1 - \mu^2)/2]^{1/2} \begin{cases} \mu^{\beta+1} & \text{if } \beta > 0 \\ \mu^{-\beta} & \text{if } \beta \leqslant 0 \end{cases} \tag{8c}$$

$$q_\beta^{2S} = p\nu^{|\beta|} \tag{8d}$$

where κ, λ, μ and ν are extension parameters of the particle wavefunctions and the displacement fields, respectively, with $0 \leqslant \kappa, \lambda, \mu, \nu \leqslant 1$, and q and p are the maximum oscillator displacements. During the following considerations we are mostly interested in the ground state and thus adopt $k = 0$ in equation (6). The wavefunction Ψ_α^{1S} is a product wavefunction with a centre of inversion between the oscillators α and $\alpha + 1$, i.e. at the tight-binding particle state φ_α. Therefore we call it a particle-centred wavefunction. Conversely Ψ_α^{2S} is a product wavefunction with an inversion centre at oscillator α and hence may be called oscillator-centred. Since the particle amplitude has maximum amplitude on the two neighbouring interstitial sites α and $\alpha + 1$, we shall also use the

name two-site (2S) wavefunction in contrast to one-site (1S) wavefunction for Ψ_α^{1S}. For the particle wavefunction amplitudes c_β^x and the oscillator displacements q_β^x we have used the geometric approach, which has proved to provide good results for the MCM (part I) and allows one to evaluate analytically the matrix elements appearing in the total energy expression

$$\varepsilon = \frac{\langle\Psi|H|\Psi\rangle}{\langle\Psi|\Psi\rangle} = \Bigg[c^2\left(\langle\Psi_0^{1S}|H|\Psi_0^{1S}\rangle + 2\sum_{\alpha=0}^{\infty}\langle\Psi_0^{1S}|H|\Psi_\alpha^{1S}\rangle\right)$$

$$+ s^2\left(\langle\Psi_0^{2S}|H|\Psi_0^{2S}\rangle + 2\sum_{\alpha=0}^{\infty}\langle\Psi_0^{2S}|H|\Psi_\alpha^{2S}\rangle\right) + cs\sum_{\alpha=0}^{\infty}\langle\Psi_0^{1S}|H|\Psi_\alpha^{2S}\rangle\Bigg]$$

$$\times\Bigg[c^2\left(\langle\Psi_0^{1S}|\Psi_0^{1S}\rangle + 2\sum_{\alpha=0}^{\infty}\langle\Psi_0^{1S}|\Psi_\alpha^{1S}\rangle\right)$$

$$+ s^2\left(\langle\Psi_0^{2S}|\Psi_0^{2S}\rangle + 2\sum_{\alpha=0}^{\infty}\langle\Psi_0^{2S}|\Psi_\alpha^{2S}\rangle\right) + cs\sum_{\alpha=0}^{\infty}\langle\Psi_0^{1S}|\Psi_\alpha^{2S}\rangle\Bigg]^{-1}. \tag{9}$$

The evaluation is performed in the Appendix. Since the summations with respect to α cannot be performed analytically the variation of the total energy with respect to the variational parameters has in general to be performed by numerical means. Before doing this we shall investigate some limiting cases.

3.1. The adiabatic limit

The adiabatic limit is the limit of nearly static, but possibly quite extended polarons for which the terms with $\alpha \neq 0$, i.e. the coherent or dynamic terms, do not contribute substantially to the total energy. In this limit the 1S and 2S solutions may be treated separately. Within the adiabatic approximation the variation with respect to the q_β^x can be performed easily yielding

$$q_\beta^x = A\left[(c_\beta^x)^2 + (c_{\beta-1}^x)^2\right] \tag{10}$$

i.e. the oscillator β relaxes due to the forces exerted by the particle occupying the two adjacent interstitial sites. Using this for the 1S solutions we have $\kappa = \lambda^2$ and $q = A(1-\kappa)$ and the energy functional takes the form

$$\varepsilon_{ad}^{1S} = -A^2[(1-\lambda^2)/(1+\lambda^2)] - 2J[2\lambda/(1+\lambda^2)]. \tag{11}$$

The variation with respect to λ can be performed in closed form, leading to

$$\lambda = (1 + A^4/4J^2)^{1/2} - A^2/2J \tag{12a}$$

and

$$E_{ad}^{1S} = -(4J^2 + A^4)^{1/2}. \tag{12b}$$

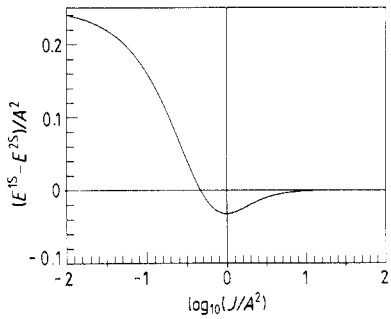

Figure 2. Energy difference $E_{ad}^{1S} - E_{ad}^{2S}$ of the adiabatic 1S and 2S solutions.

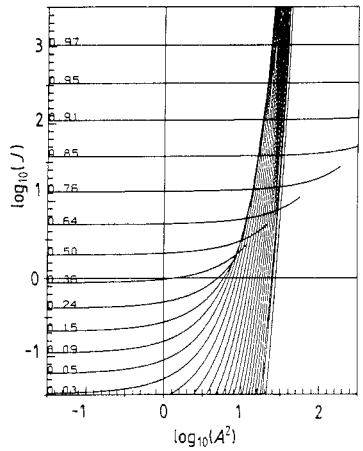

Figure 3. Curves of κ = constant for the dynamic solutions.

Using equation (10) we find for the adiabatic 2S solutions the expressions $\nu = \mu^2$, $p = A(1 - \nu)$ and

$$\varepsilon_{ad}^{2S} = -\tfrac{1}{4}A^2(3 - 4\mu^2 - \mu^4) - J(1 + 2\mu - \mu^2). \tag{13}$$

Here the variation with respect to μ cannot be done analytically in general. For small polarons ($J/A^2 \ll 1$)

$$E_{ad}^{2S} = -A^2(\tfrac{3}{4} + J/A^2 + J^2/A^4) \tag{14a}$$

can be derived. Comparing this with the corresponding expression

$$E_{ad}^{1S} = -A^2(1 + 2J^2/A^4)$$

for the 1S solution, the 2S solution turns out to be unfavourable in the small-polaron limit. On the other hand in the limit $J/A^2 \gg 1$ we find

$$E_{ad}^{2S} = -2J - A^4/4J - A^6/8J^2 \tag{14b}$$

which may be compared with

$$E_{ad}^{1S} = -2J - A^4/4J - A^8/64J^3$$

for the 1S solutions. Here both first-order corrections are equal but the 2S solution is favourable due to the second-order term. In figure 2 the energy difference $E_{ad}^{1S} - E_{ad}^{2S}$ is plotted as a function of J/A^2. It can be seen that the 1S solutions have lower energy up to $J/A^2 = 0.466$. For larger values of J/A^2 the 2S solutions are favourable. Since for $J/A^2 = 0.466$, $\mu \simeq 0.25$ holds, the transition may be said to take place in the small-polaron region. The reason for the stabilisation of the 2S solutions is the more effective tunnelling in these states, which for increasing J/A^2 overcompensates the slightly worse relaxation of the lattice.

3.2. The dynamic approximation

In the dynamic approximation we assume that the particle wavefunction is concentrated at a single site, i.e. $c_\beta^\varkappa = \delta_{\beta,0}$, while the displacement field is geometrically decreasing

around the occupied interstitial site. Obviously due to this definition only dynamic 1S solutions can exist. The energy functional for these reads

$$\varepsilon_{\text{dyn}} = \frac{q^2}{1-\kappa^2} - 2Aq - 2J\exp\left(-\frac{q^2}{2}\frac{1-\kappa}{1+\kappa}\right). \tag{15}$$

Variation with respect to q and κ yields

$$q = A(1-\kappa) \tag{16a}$$

$$J = \frac{\kappa}{(1-\kappa)^2}\exp\left(\frac{A^2}{2}\frac{(1-\kappa)^3}{1+\kappa}\right) \tag{16b}$$

and the implicit expression for the energy

$$E_{\text{dyn}} = -A^2\frac{1-\kappa}{1+\kappa}(1+2\kappa) - 2\frac{\kappa}{(1-\kappa)^2}. \tag{17}$$

These are minima when

$$A^2 < \left(\frac{1+\kappa}{1-\kappa}\right)^3\frac{1}{\kappa(2+\kappa)}. \tag{18}$$

The curves of solutions $J(\kappa, A)$ according to equation (16) are plotted in figure 3. The results are very similar to those derived for the MCM in part I. The limiting expressions for the energies of small and large dynamic polarons are

$$E_{\text{dyn}} = -A^2 - 2J\exp(-\tfrac{1}{2}A^2) \tag{19}$$

and

$$E_{\text{dyn}} = -2J - A^2J^{-1/2} \tag{20}$$

respectively.

3.3. General numerical variation

Having treated the limiting cases to be expected we now turn to the general numerical variation of the energy functional. Apart from the two model parameters J and A^2, the energy functional (equation (9)) contains $s, \kappa, \lambda, \mu, \nu, p$ and q as independent variational parameters. Without loss of generality, c may be set to $(1-s^2)^{1/2}$. To reduce the number of parameters we approximate q by $A(1-\kappa)$ and p by $A(1-\nu)$. This approximation is suggested by the limiting cases discussed above. Hence we are left with a five-parameter variational problem. We solved it on a computer using the above-mentioned limiting solutions as starting points of a gradient procedure. The results are shown in figure 4. As descriptors for the ground-state properties the 2S portion s^2 as well as the mean polaron extension parameter $\kappa \equiv c^2\kappa + s^2\nu$ and the mean adiabaticity parameter $\eta \equiv c^2\lambda^2/\kappa + s^2\mu^2/\nu$ are displayed as functions of J and A^2. Furthermore the boundary lines $s^2 = 0.5$, $\kappa = 0.5$ and $\eta = 0.5$ are displayed in figure 4(d) to provide a synopsis of the three parameters.

Let us first consider figure 4(d) to give a rough classification of the most important regions. As in the MCM we find a region of dynamic large-polaron solutions in the upper left corner of the diagram, i.e. for $J \gg \max(A^2, 1)$. As previously mentioned these solutions are purely of 1S type. Moving anticlockwise through the diagram we then reach

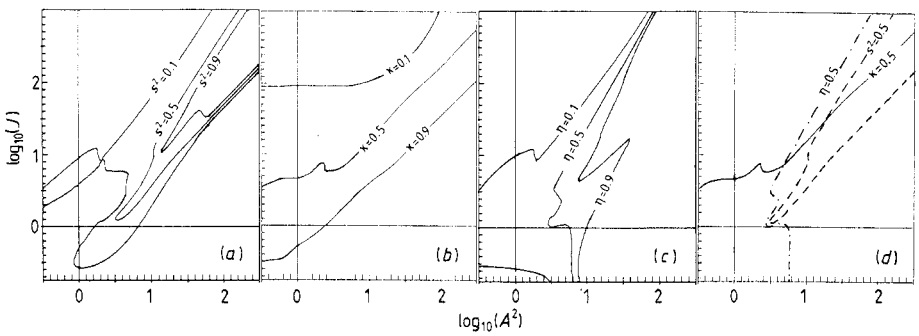

Figure 4. Diagrams of the polaronic ground-state properties: (*a*) 2S portion s^2; (*b*) mean polaron extension parameter κ; (*c*) mean adiabaticity parameter η; and (*d*) synopsis of the lines $s^2 = 0.5$, $\kappa = 0.5$ and $\eta = 0.5$.

a region of small dynamic solutions which continuously turns over to the small adiabatic 1S solutions in the lower right corner. At the line $J = 0.466A^2$ the ground state takes the form of adiabatic 2S solutions which can be considered as relatively small polarons since the extension parameter ν ranges from 0.1 to 0.7 in the 2S region. Finally a narrow area of intermediate 1S solutions can be found between the adiabatic 2S region and the dynamic 1S region. These intermediate solutions behave like large adiabatic solutions even though the fundamental condition of adiabaticity does not hold. Their nature is discussed in part I in some detail.

Let us now look at the more sophisticated features appearing in figure 4. Mostly there is quite a large distance between the lines $s^2 = 0.1$ and $s^2 = 0.5$ in figure 4(*a*). This clearly shows that a small coherent admixture of 2S solutions to the 1S solutions is favourable in a wide parameter range. This feature is pronounced in the region of adiabatic 1S solutions where a bank of 2S admixture can be observed not only along the borderline of the region in the large-polaron area but also forming an island within the dynamic region in the transition area from large to small dynamic solutions. The exact coincidence of the lines $s^2 = 0.1$ and $\eta = 0.1$ along these banks strongly indicates that the beginning of the 2S admixture is more discontinuous than smooth. The transition from adiabatic 1S polarons to adiabatic 2S polarons along the line $J = 0.466A^2$ appears to be discontinuous for $A^2 > 65$ while it is quite smooth for smaller values of A^2. Looking in more detail at figure 4(*c*) we clearly see a smooth increase in the adiabaticity η during the transition from small dynamic to small adiabatic 1S solutions.

The transition from the 2S solutions to the intermediate 1S solutions is continuous as indicated by the behaviour of the lines $s^2 = 0.9$ and $s^2 = 0.5$ in the entire region. On the other hand, from the behaviour of the $\eta = 0.5$ and $\eta = 0.9$ lines, the crossover from the intermediate solutions to the dynamic solutions appears to be sharp, at least for $A^2 > 30$. This borderline is approximately described by $J \simeq 0.18A^2$. This seems to be reasonable since a similar power law, namely $J \simeq 0.03A^2$, has been observed within the MCM.

Finally in the parameter area $J \simeq A^2 \simeq 0.5$ a most complicated mixing of all limiting types of solutions takes place, which cannot be described here in detail.

By performing the same variational procedure for a small non-zero value of k in equation (6) the effective mass m^{**} of the polaron ground state has been calculated as

$$m^{**} = k^2/2[E(k) - E(k = 0)]. \tag{21}$$

This may be compared with the effective mass $m^* = 1/(2J)$ of the particle in a rigid-

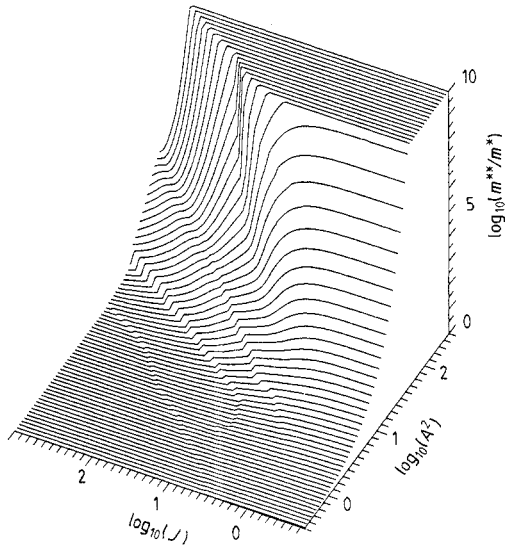

Figure 5. Relief diagram of the polaronic effective mass.

lattice tight-binding treatment. In figure 5 a relief diagram of $\log_{10}(m^{**}/m^*)$ is shown. The areas of different polaronic ground states may be easily recognised. Especially the discontinuous crossover lines appear as steps in this diagram. Thus the transition from the intermediate to the dynamic solutions turns out to be discontinuous even for $A^2 < 30$.

4. Configuration-dependent transfer integral

Within the MCM as well as hitherto in the IPM the Condon approximation (CA) has been adopted, i.e. the transfer integral J was assumed to be independent of the actual configuration of the lattice. For atom- or molecule-centred tight-binding states there is little known about the goodness of the CA. Thus it might be justifiable within the MCM. Its validity, however, must not be taken for granted. On the other hand the CA can be seen to be poor in the case of the IPM by a glance at figure 1(*b*). The two atoms of each oscillator can be assumed to form a bottleneck, i.e. a potential barrier, for the particle. This barrier will be lowered by an elongation of the spring, i.e. by a positive displacement of the oscillator, and vice versa. Since the transfer integral between two adjacent interstitial sites is extremely sensitive to the barrier height, it depends strongly on the displacement of the entire oscillator. Such a configuration dependence of the transfer integral has been shown to be of considerable importance for the dynamics of hydrogen in metals (Klamt and Teichler 1986). These results as well as fundamental quantum mechanics strongly suggest the configuration dependence to be of exponential form. Therefore we shall investigate the consequences of a configuration-dependent transfer integral given by

$$J_\alpha = J \exp[(g/A)Q_\alpha] \tag{22}$$

throughout this chapter.

By the afore-mentioned arguments the sign of the dimensionless parameter g clearly appears to be positive, while no general estimation of its magnitude can be given. The particle Hamiltonian now takes the form

$$H_P = -J\sum_\alpha \exp[(g/A)Q_\alpha](a_\alpha^+ a_{\alpha+1} + a_\alpha^+ a_{\alpha+1}). \tag{23}$$

The evaluation of the entire matrix element now gives (see Appendix)

$$\langle\Psi_0^x|H_P|\Psi_\alpha^y\rangle = -\tilde{J}\exp(-S_\alpha^{xy}) \times \sum_\beta \exp[(g/A)(q_\beta^x + q_{\beta-\alpha}^y)](c_\beta^x c_{\beta-\alpha+1}^y + c_{\beta+1}^x c_{\beta-\alpha}^y) \tag{24}$$

where $\tilde{J} \equiv J\exp(\frac{1}{4}g^2/A^2)$ is the expectation value of the transfer integral in the oscillator ground-state. To make the summation with respect to β feasible we restrict ourselves further to the zero- and first-order terms with respect to g yielding

$$\langle\Psi_0^x|H_P|\Psi_\alpha^y\rangle = -\tilde{J}\exp(-S_\alpha^{xy}) \times \sum_\beta [1 + (g/A)(q_\beta^x + q_{\beta-\alpha}^y)](c_\beta^x c_{\beta-\alpha+1}^y + c_{\beta+1}^x c_{\beta-\alpha}^y). \tag{25}$$

Together with all other sums the new type of sum has been evaluated in the Appendix for the geometrical approach given in equations (8) and (9) with the only modification that $r \equiv q_0^{2S}$ is treated as a separate variational parameter.

4.1. Adiabatic solutions

Again we shall first investigate the adiabatic solutions. Within the adiabatic approximation variation with respect to the q_β^x easily yields the expressions

$$\kappa = \lambda^2 \tag{26}$$

$$q = A[1 + 2gz\lambda/(1+\lambda^2)](1-\lambda^2) \tag{27}$$

$$\nu = \mu^2 \tag{28}$$

$$p = \tfrac{1}{2}(1+\mu^2)A(1+\mu^2+2gz\mu) \tag{29}$$

and

$$r = (1-\mu^2)A(1+zg) \tag{30}$$

where the abbreviation $z = \tilde{J}/A^2$ has been introduced. The energy functionals for the 1S and 2S solutions now become

$$\varepsilon_{ad}^{1S} = -A^2\left[4z\frac{\lambda}{1+\lambda^2} + \left(1 + 2\frac{gz\lambda}{1+\lambda^2}\right)^2\frac{1-\lambda^2}{1+\lambda^2}\right] \tag{31}$$

and

$$\varepsilon_{ad}^{2S} = -A^2[\tfrac{1}{4}(1-\mu^2)(3-\mu^2) + gz(1-\mu^2)(1+\mu-\mu^2) + \tfrac{1}{2}zg^2(1+2\mu-\mu^4)(1-\mu^2)/(1+\mu^2) + z(1+2\mu-\mu^2)] \tag{32}$$

respectively. The variation with respect to λ and μ has to be performed numerically. The

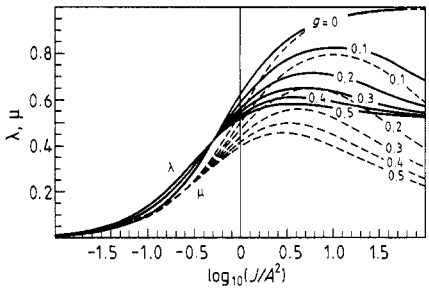

Figure 6. Wavefunction extension parameters λ and μ of the adiabatic 1S and 2S solutions, respectively, for six values of the configuration dependence g.

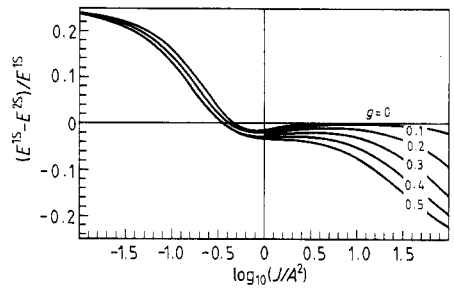

Figure 7. Relative energy difference $(E_{ad}^{1S} - E_{ad}^{2S})/E_{ad}^{1S}$ of the adiabatic 1S and 2S solutions for six values of g.

results are plotted in figures 6 and 7 for g varying in the range 0.0 to 0.5. Figure 7 shows the behaviour of the wavefunction extension parameters λ and μ. For small values of z only a slight increase of λ and μ is effected by the non-zero values of g. On the other hand for $z \gg 1$ and $g > 0$, λ and μ no longer tend to one: λ can be shown to become 0.52 for $z \to \infty$ while μ even tends to zero. Thus we may state as an important effect of the configuration dependence that it inhibits the appearance of large adiabatic polarons. In figure 7 the relative energy difference $(E_{ad}^{1S} - E_{ad}^{2S})/E_{ad}^{1S}$ is drawn as a function of z. In general the 2S solutions can be seen to take greater advantage of the configuration dependence. The transition point from 1S to 2S solutions moves slightly towards smaller values of z for increasing g, but the more drastic effect is the large energy gain of the 2S solutions at large values of z.

4.2. Dynamic solutions

Within the dynamic approximation the energy functional takes the form

$$\varepsilon_{dyn} = \frac{q^2}{1-\kappa^2} - 2Aq - 2\tilde{J}\left(1+\frac{g}{A}q\right)\exp\left(-\frac{q^2}{2}\frac{1-\kappa}{1+\kappa}\right). \tag{33}$$

It can easily be seen that in the small-polaron limit the configuration dependence is equivalent to an increase in the transfer integral J by a factor $(1 + g)$, while in the large-polaron limit it acts like an increase in the interaction A by a factor $(1 + J/A^2)$.

4.3. Numerical calculations

Since the numerical variation of the energy functional is very time-consuming we content ourselves here with the calculation of the energetic minimum of the three basic types of solutions, i.e. the adiabatic 1S and 2S solutions and the dynamic solutions. The borderlines between the solution types are plotted in figure 8 for four values of g. Figure 8(a) reveals the situation for $g = 0$ and thus corresponds to figure 5(d). The 2S region appears as a narrow wedge in the upper right corner. Figures 8(b)–(d) show the effects of a configuration-dependent transfer integral for $g = 0.1$, $g = 0.3$ and $g = 0.5$, respectively. As previously mentioned with increasing g the borderline between adiabatic 1S and 2S solutions moves slightly in favour of the latter. In contrast the boundary between adiabatic 2S solutions and dynamic solutions bends strongly even for relatively small

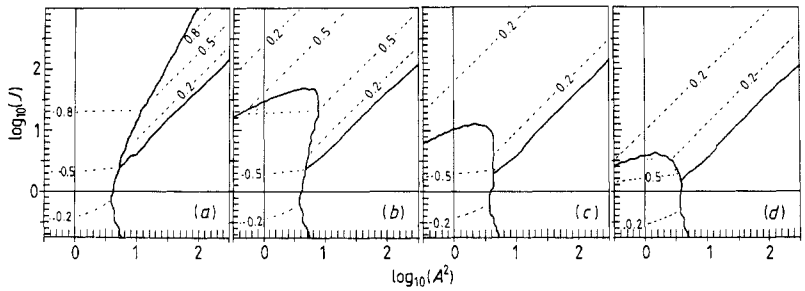

Figure 8. Borderlines of the three basic types of solutions together with the lines $\kappa = 0.2$, 0.5 and 0.8 of the mean polaron extension parameter for four values of g.

values of g. In the region originally occupied by large dynamic solutions we now find adiabatic 2S polarons with limited and even decreasing extension for large values of $\tilde{J}/A^2$ as has been shown in § 4.1. The borderline between the dynamic and adiabatic 1S solutions is nearly unaffected by g. We may thus state that the most important effect of a positive configuration dependence g of the transfer integral is the inhibition of large dynamic polarons by the appearance of relatively localised 2S solutions.

5. Summary and discussion

In the present paper the polaronic behaviour of interstitial particles has been investigated for the first time. The appearance of 2S solutions with equal maximal amplitude of the particle wavefunction on two neighbouring interstitial sites has turned out to be the most important change in the polaronic solution spectrum of the IPM compared with the MCM. Even though the existence of analogous more-site states of interstitial particles has been proposed before in the context of hydrogen in metals (Sugimoto and Fukai 1981, Klamt and Teichler 1986) here for the first time they are embedded within a consistent polaron model and thus the conditions for the stability of such solutions could be derived. Thus the understanding of this particular type of solutions in comparison with one-site solutions and with extended band-like solutions could be improved.

Furthermore for the first time a polaron model has been extended beyond the Condon approximation, i.e. a configuration dependence of the transfer integral has been taken into account. An increase of the transfer integral with a widening of the bottleneck between two interstitial sites, which appears to be likely for interstitial particles, is shown to increase the importance of the 2S solutions drastically. These solutions now show the strange feature of localisation with increasing transfer integral, since it turns out to become more effective to widen a limited crystal region and thereby increase the effective transfer integral in this region considerably than to increase the gain in kinetic energy by delocalisation over a large crystal volume.

The results of this paper are of some importance for the understanding of the states and the dynamics of light positively charged particles in metals as there are positrons, positive muons and pions and the three hydrogen nuclei protons, deuterons and tritons in order of increasing mass. The result of increasing stability and localisation of more-site states with increasing transfer integral raises the question whether the states of lighter particles are more extended or perhaps more localised than those of heavier ones. Thus even the self-trapping of positrons in metals appears to be realistic. In general the

strong dependence of the polaronic ground state on the entire parameters A and J, which are likely to vary considerably with the particle mass, makes the interpolation and extrapolation of polaronic properties within the above-mentioned series of particles much more complicated than usually assumed. The various different possibilities for the type of the polaronic ground state should be taken into account in the interpretation of all experiments of light positively charged particles especially if questions of coherence are concerned.

Appendix

The matrix elements $\langle\Psi_0^x|\Psi_\alpha^y\rangle$ and $\langle\Psi_0^x|H|\Psi_\alpha^y\rangle$ may be evaluated in much the same way as has been shown in the Appendix of part I. We thus find

$$\langle\Psi_0^x|\Psi_\alpha^y\rangle = \sum_\beta c_\beta^x c_{\beta+\alpha}^y \exp(-S_\alpha^{xy})$$

and

$$\begin{aligned}\langle\Psi_0^x|H|\Psi_\alpha^y\rangle = \exp(-S_\alpha^{xy}) \Bigg(& \tfrac{1}{2}\sum_\gamma q_\gamma^x q_{\gamma-\alpha}^y \sum_\beta c_\beta^x c_{\beta-\alpha}^y \\ & - \tfrac{1}{2}\sum_\beta c_\beta^x c_{\beta-\alpha}^y (q_\beta^x + q_{\beta-1}^x + q_\beta^y + q_{\beta-1}^y) \\ & - J\exp(g^2/4A^2)\sum_\beta \exp[(g/2A)(q_\beta^x + q_{\beta+\alpha}^y)] \\ & \times (c_\beta^x c_{\beta-\alpha+1}^y + c_{\beta+1}^x c_{\beta-\alpha}^y)\Bigg)\end{aligned}$$

where

$$S_\alpha^{xy} = \tfrac{1}{4}\sum_\beta (q_\beta^x - q_{\beta-\alpha}^y)^2.$$

Here the most general form of the Hamiltonian, i.e. H_P according to equation (24), has been used. Results suitable for § 2 may be derived by setting $g = 0$. For the sake of getting closed expressions we use the approximation

$$\exp[(g/2A)(q_\beta^x + q_{\beta+\alpha}^y)] \simeq [1 + (g/2A)(q_\beta^x + q_{\beta+\alpha}^y)].$$

Furthermore we shall use the most general form of the geometric approach, i.e. q_β^x and c_β^x according to equation (8) apart from $q_0^{2S} = r$ instead of p, in the subsequent evaluation of the sums. Thus here the results used in § 2 may be found by replacing r by p.

With these agreements all the different sums may be evaluated without problems but with considerable effort, yielding the following results:

$$S_\alpha^{1S1S} = \tfrac{1}{2}q^2\left(2\frac{1-\kappa^\alpha}{1-\kappa^2} - \frac{\alpha}{\kappa}\kappa^\alpha\right)$$

$$\begin{aligned}S_\alpha^{1S2S} = \tfrac{1}{2}\Bigg\{ & \frac{r^2}{2} + \frac{p^2}{1-\nu^2} + \frac{q^2}{1-\kappa^2} - q\left[\left(r + \frac{p\kappa}{1-\nu\kappa} + \frac{p}{\kappa-\nu}\right)\kappa^\alpha \right. \\ & \left. + p\left(\frac{1}{1-\nu\kappa} - \frac{1}{\kappa-\nu}\right)\nu^\alpha\right]\Bigg\}\end{aligned}$$

$$S_0^{2S2S} = \begin{cases} \frac{1}{2}\{r^2 + p^2[2(1-\nu^\alpha)/(1-\nu^2) - (\alpha-1)\nu^{\alpha-2}] - 2pr\nu^{\alpha-1}\} & \text{if } \alpha > 0 \\ 0 & \text{if } \alpha = 0 \end{cases}$$

$$\sum_\beta c_\beta^{1S} c_{\beta-\alpha}^{1S} = (c_0^{1S})^2 \left(\frac{1+\lambda^2}{1-\lambda^2} + \alpha\right) \lambda^\alpha$$

$$\sum_\beta c_\beta^{1S} c_{\beta-\alpha}^{2S} = c_0^{1S} c_0^{2S} \left[\left(\frac{\lambda}{1-\mu\lambda} + \frac{\lambda}{\lambda-\mu}\right) \lambda^\alpha + \left(\frac{1}{1-\mu\lambda} - \frac{1}{\lambda-\mu}\right) \mu^\alpha\right]$$

$$\sum_\beta c_\beta^{2S} c_{\beta-\alpha}^{2S} = (c_0^{2S})^2 \left(\frac{2}{1-\mu^2} + \frac{\alpha}{\mu}\right) \mu^\alpha$$

$$\sum_\beta q_\beta^{1S} q_{\beta-\alpha}^{1S} = q^2 \left(\frac{2}{1-\kappa^2} + \frac{\alpha}{\kappa}\right) \kappa^\alpha$$

$$\sum_\beta q_\beta^{1S} q_{\beta-\alpha}^{2S} = qr\kappa^\alpha + qp \left(\frac{\kappa^\alpha - \nu^\alpha}{\kappa-\nu} + \frac{\kappa^{\alpha+1} + \nu^\alpha}{1-\kappa\nu}\right)$$

$$\sum_\beta q_\beta^{2S} q_{\beta-\alpha}^{2S} = \begin{cases} r^2 + 2p^2/(1-\nu^2) & \text{if } \alpha = 0 \\ \{2r\nu + p[\alpha - 1 + 2\nu^2/(1-\nu^2)]\}q & \text{if } \alpha > 0 \end{cases}$$

$$\sum_\beta c_\beta^{1S} c_{\beta-\alpha}^{1S} (q_\beta^{1S} + q_{\beta+1}^{1S}) = q\lambda^\alpha \left(\frac{1+\lambda^2\kappa^\alpha + \lambda^2 + \kappa^\alpha}{1-\kappa\lambda^2} + 2\frac{1-\kappa^\alpha}{1-\kappa}\right)$$

$$\begin{aligned} \tfrac{1}{2}\sum_\beta c_\beta^{1S} c_{\beta-\alpha}^{2S} (q_\beta^{1S} + q_{\beta+1}^{1S} + q_\beta^{2S} + q_{\beta+1}^{2S}) &= \frac{r}{2}(1+\lambda)\lambda^\alpha + \frac{q}{2}\left(\frac{(1+\mu\lambda)\mu^\alpha + (1+\kappa)\kappa^\alpha\lambda^{\alpha+1}}{1-\kappa\mu\lambda}\right. \\ &\quad \left. + \frac{(1+\kappa)\kappa^\alpha\lambda^{\alpha+1} - (\mu+\lambda)\mu^\alpha}{\kappa\lambda - \mu}\right) \\ &\quad + \frac{p}{2}\left(\frac{\lambda^{\alpha+1} + \mu^\alpha\nu^\alpha}{1-\nu\mu\lambda}(1+\mu\lambda) + \frac{\lambda^\alpha + \mu^\alpha\nu^\alpha}{\lambda-\mu\nu}(\mu+\lambda)\right) \end{aligned}$$

$$\sum_\beta c_\beta^{2S} c_{\beta-\alpha}^{2S} (q_\beta^{2S} + q_{\beta+1}^{2S}) = \begin{cases} \mu^\alpha \left[\left(\frac{1+\mu^2+\nu^{\alpha-1}(1+\mu)}{1-\nu\mu^2} + \frac{2-\nu^{\alpha-1}(1+\nu)}{\mu(1-\nu)}\right) p + r\frac{1+\mu}{\mu}\right] & \text{if } \alpha > 0 \\ 2\left(\frac{1+\mu^2}{1-\nu\mu^2}p + r\right) & \text{if } \alpha = 0 \end{cases}$$

$$\sum_\beta c_\beta^{1S} c_{\beta-\alpha+1}^{1S} + c_{\beta+1}^{1S} c_{\beta-\alpha}^{1S} = \lambda^\alpha \frac{4\lambda}{1-\lambda^2} + \alpha\lambda^{\alpha-1}(1+\lambda^2)$$

$$\begin{aligned} &\sum_\beta c_\beta^{1S} c_{\beta-\alpha+1}^{2S} + c_{\beta+1}^{1S} c_{\beta-\alpha}^{2S} \\ &\quad = \frac{\lambda^\alpha(1+\lambda^2) + \mu^\alpha\lambda(1+\mu^2)}{1-\mu\lambda} + \frac{\lambda^\alpha(1+\lambda^2) - \mu^\alpha(1+\mu^2)}{\lambda-\mu} \end{aligned}$$

$$\sum_\beta c_\beta^{2S} c_{\beta-\alpha+1}^{2S} + c_{\beta+1}^{2S} c_{\beta-\alpha}^{2S}$$

$$= \begin{cases} \mu^{\alpha-2}[2\mu(1+\mu^2)/(1-\mu^2) - 1 + \mu^2 + \alpha(1+\mu^2)] & \text{if } \alpha > 0 \\ 2[1 + 2\mu/(1-\mu^2)] & \text{if } \alpha = 0 \end{cases}$$

$$\sum_\beta q_\beta^{1S}(c_\beta^{1S} c_{\beta-\alpha+1}^{1S} + c_{\beta+1}^{1S} c_{\beta-\alpha}^{1S}) = q\left(2\lambda \frac{1+\kappa^\alpha}{1-\kappa\lambda^2} + \frac{(1-\kappa^\alpha)(1+\lambda^2)}{\lambda(1-\kappa)}\right)\lambda^\alpha$$

$$\tfrac{1}{2}\sum_\beta (q_\beta^{1S} + q_\beta^{2S})(c_\beta^{1S} c_{\beta-\alpha+1}^{2S} + c_{\beta+1}^{1S} c_{\beta-\alpha}^{2S})$$

$$= \begin{cases} \dfrac{q}{2}\left(\dfrac{(1+\kappa\lambda^2)\kappa^\alpha\lambda^\alpha + (\mu+\lambda)\mu^\alpha}{1-\kappa\lambda\mu} + \dfrac{(1+\kappa\lambda^2)\kappa^\alpha\lambda^\alpha - (1+\mu\lambda)\mu^\alpha}{\kappa\lambda - \mu}\right) \\ \qquad + \dfrac{r}{2}(1+\lambda)\lambda^\alpha + \dfrac{p}{2}\left(\dfrac{(1+\nu\mu)\nu^\alpha\mu^\alpha + (\mu+\lambda)\lambda^\alpha}{1-\nu\lambda\mu}\lambda\right. \\ \qquad \left. + \dfrac{\lambda^\alpha(1+\mu\lambda) - \mu^\alpha\nu^\alpha(1+\nu\mu)}{\lambda-\mu\nu}\right) & \text{if } \alpha > 0 \\ \dfrac{q}{2}\left(\lambda + \dfrac{1+\mu+\lambda+\kappa\lambda^2}{1-\kappa\mu\lambda}\right) + \dfrac{p}{2}\dfrac{(1+\lambda)(\mu+\lambda)}{1-\nu\mu\lambda} + \dfrac{r}{2}(1+\lambda) & \text{if } \alpha = 0 \end{cases}$$

$$\sum_\beta q_\beta^{2S}(c_\beta^{2S} c_{\beta-\alpha+1}^{2S} + c_{\beta+1}^{2S} c_{\beta-\alpha}^{2S})$$

$$= \begin{cases} \mu^{\alpha-2}\left[p\left(\mu\dfrac{2\mu^2 + (\mu^2\nu+1)\nu^{\alpha-1}}{1-\nu\mu^2} + \dfrac{(1+\mu^2) - (\mu^2\nu+1)\nu^{\alpha-1}}{1-\nu}\right)\right. \\ \qquad \left. + r\mu(1+\mu)\right] & \text{if } \alpha > 0 \\ 2\left(\dfrac{2\mu p}{1-\nu\mu^2} + r\right) & \text{if } \alpha = 0 \end{cases}$$

References

Alefeld G and Voelkl J 1978 *Hydrogen in Metals* vol 1 (Berlin: Springer)
Holstein T 1959a *Ann. Phys., NY* **8** 325
—— 1959b *Ann. Phys., NY* **8** 343
Klamt A 1988 *J. Phys. C: Solid State Phys.* **21** 1953
Klamt A and Teichler H 1986 *Phys. Status Solidi* b **134** 533
Richter D 1986 *Springer Proceedings in Physics* vol 17 (Berlin: Springer) p 140
Sugimoto H and Fukai Y 1981 *J. Phys. Soc. Japan* **50** 3709